

The Catalytic and GAF Domains of the Rod cGMP Phosphodiesterase (PDE6) Heterodimer Are Regulated by Distinct Regions of Its Inhibitory γ Subunit*

Received for publication, April 13, 2001, and in revised form, May 11, 2001
Published, JBC Papers in Press, May 24, 2001, DOI 10.1074/jbc.M103316200

Hongmei Mou and Rick H. Cote \ddagger

From the Department of Biochemistry and Molecular Biology, University of New Hampshire, Durham, New Hampshire 03824-2617

The central effector of visual transduction in retinal rod photoreceptors, cGMP phosphodiesterase (PDE6), is a catalytic heterodimer ($\alpha\beta$) to which low molecular weight inhibitory γ subunits bind to form the nonactivated PDE holoenzyme ($\alpha\beta\gamma_2$). Although it is known that γ binds tightly to $\alpha\beta$, the binding affinity for each γ subunit to $\alpha\beta$, the domains on γ that interact with $\alpha\beta$, and the allosteric interactions between γ and the regulatory and catalytic regions on $\alpha\beta$ are not well understood. We show here that the γ subunit binds to two distinct sites on the catalytic $\alpha\beta$ dimer ($K_{D1} < 1$ pM, $K_{D2} = 3$ pM) when the regulatory GAF domains of bovine rod PDE6 are occupied by cGMP. Binding heterogeneity of γ to $\alpha\beta$ is absent when cAMP occupies the noncatalytic sites. Two major domains on γ can interact independently with $\alpha\beta$ with the N-terminal half of γ binding with 50-fold greater affinity than its C-terminal, inhibitory region. The N-terminal half of γ is responsible for the positive cooperativity between γ and cGMP binding sites on $\alpha\beta$ but has no effect on catalytic activity. Using synthetic peptides, we identified regions of the amino acid sequence of γ that bind to $\alpha\beta$, restore high affinity cGMP binding to low affinity noncatalytic sites, and retard cGMP exchange with both noncatalytic sites. Subunit heterogeneity, multiple sites of γ interaction with $\alpha\beta$, and positive cooperativity of γ with the GAF domains are all likely to contribute to precisely controlling the activation and inactivation kinetics of PDE6 during visual transduction in rod photoreceptors.

The extent and lifetime of activation of the photoreceptor cGMP PDE¹ (PDE6; EC 3.1.4.35) must be precisely regulated in rod and cone cells to control the exquisite sensitivity, speed, and adaptational properties of the visual transduction pathway

* This work was supported by National Institutes of Health Grant EY-05798 (to R. H. C.). This paper is Scientific Contribution Number 2088 from the New Hampshire Agricultural Experiment Station. The costs of publication of this article were defrayed in part by the payment of page charges. This article must therefore be hereby marked "advertisement" in accordance with 18 U.S.C. Section 1734 solely to indicate this fact.

\ddagger To whom correspondence should be addressed: Dept. of Biochemistry and Molecular Biology, University of New Hampshire, 46 College Rd., Durham, NH 03824-2617. Tel.: 603-862-2458; Fax: 603-862-4013; E-mail: rick.cote@unh.edu.

¹ The abbreviations used are: PDE, cyclic nucleotide phosphodiesterase; LY, Lucifer Yellow; GTP γ S, guanosine 5'-3-O-(thio)triphosphate; P $\alpha\beta$, catalytic heterodimer of PDE6; P γ , 10-kDa inhibitory γ subunit of rod PDE6; K_D , dissociation constant; K_m , Michaelis constant; k_{cat} , catalytic; K_i , inhibition constant; GAF, a protein domain named for its occurrence in cGMP-regulated phosphodiesterases, Adenyl cyclases, and the *E. coli* protein, FhlA.

in vertebrate photoreceptors. The membrane-associated rod photoreceptor PDE6 consists of a dimer of two homologous catalytic subunits (P $\alpha\beta$) to which two low molecular weight inhibitory subunits (P γ) bind (holoenzyme stoichiometry, $\alpha\beta\gamma_2$). The catalytic subunits contain GAF domains that are responsible for high affinity, noncatalytic binding of two cGMP molecules/holoenzyme. It is well established that relief of the inhibitory constraint on PDE6 arises from the binding of activated heterotrimeric G protein (transducin) to P γ following photoactivation of the visual pigment, rhodopsin (reviewed in Refs. 1–4). However, the strength of the interaction between P γ and P $\alpha\beta$ has been difficult to quantitate, and K_D values vary widely (from picomolar (5–7) up to nanomolar values (8, 9)). In addition, it has not been conclusively demonstrated whether both P γ molecules bind with equal affinity to P $\alpha\beta$ to form the nonactivated holoenzyme (although two different binding sites on P $\alpha\beta$ have been inferred using mutant P γ (10)). Finally, recent evidence suggests that binding of activated transducin to PDE6 relieves inhibition at only one of the two active sites, further supporting the idea of catalytic subunit heterogeneity with respect to P γ binding (11, 12).

Use of synthetic peptides to defined regions of P γ and mutagenesis of the P γ subunit have revealed that P γ has multiple sites of interaction with rod P $\alpha\beta$, with the α subunit of activated transducin (α_t^*), and with the RGS-9 (regulator of G protein signaling 9). The C-terminal residues of P γ (amino acids 77–87) have been shown to interact directly with the catalytic sites of P $\alpha\beta$ to inhibit catalysis (7, 13–15). A second major site of interaction between P γ and P $\alpha\beta$ has been identified in the lysine-rich central portion (amino acids 24–45) of the P γ sequence (13, 16–19), but the function of this interaction is unclear. α_t^* has been shown to interact with P γ at two distinct regions: one in its C-terminal domain (amino acid residues 65–87) and one in the central, lysine-rich region of P γ (13, 14, 16, 20–22). Finally, P γ also serves to potentiate the GTPase-activating protein function of RGS-9 by interacting with the protein in the neighborhood of Trp⁷⁰ (21–23).

In this paper, we show that the K_D of P γ binding to rod PDE6 is in the picomolar to subpicomolar range. Furthermore, P γ does not bind with equal affinity to the two sites on P $\alpha\beta$ when cGMP occupies the noncatalytic regulatory sites located on the P $\alpha\beta$ dimer. We also demonstrate that the central region of P γ stabilizes high affinity cGMP binding to the noncatalytic sites, and the affinity of the central region of P γ exceeds by 50-fold the affinity of its C-terminal region. Finally, using a series of synthetic peptides, we identify important residues in the central region that contribute to the stabilization of P γ binding to P $\alpha\beta$.

EXPERIMENTAL PROCEDURES

Materials—Bovine retinas were purchased from W. L. Lawson, Inc. The P γ mutant, P γ 1–45C (consisting of the first 45 amino acids of

bovine rod $P\gamma$ plus a C-terminal cysteine residue (24)) was a kind gift of Dr. N. P. Skiba, whereas zaprinast was generously supplied by Rhone-Poulenc Rorer (Dagenham, UK). Crude synthetic peptides were prepared at New England Peptide or at the protein facility at the University of New Hampshire. The radiochemicals were from PerkinElmer Life Sciences. Gel electrophoresis and immunoblotting supplies were from Bio-Rad. Ultima Gold scintillation fluid was from Packard Instrument Co., filtration and ultrafiltration products were from Millipore, protein assay reagents were from Pierce, and all other chemicals were from Sigma.

Preparation of PDE6—Membrane-associated bovine rod PDE6 was purified to >90% homogeneity from frozen bovine retinas as described previously (25). The resulting nonactivated PDE holoenzyme (subunit stoichiometry: $\alpha\beta\gamma_2$) was stored in 50% glycerol at -20°C . The PDE6 catalytic heterodimer ($P\alpha\beta$) was prepared by limited proteolysis of the $P\gamma$ subunits followed by Mono Q ion-exchange chromatography to remove proteolytic fragments of $P\gamma$ (25). The $P\alpha\beta$ preparation was >95% pure as judged from Coomassie-stained SDS-polyacrylamide gel electrophoresis. No shift in the apparent molecular weight of the α or β subunit was observed following this treatment. (Attempts to prepare $P\alpha\beta$ without resorting to proteolytic digestion of $P\gamma$ were unsuccessful.) Immunoblot analysis with an anti-peptide $P\gamma$ antibody (UNH9710) directed to the C-terminal region (amino acids 63–87) of $P\gamma$ revealed no detectable full-length $P\gamma$; a 5-kDa band representing the major proteolytic product of $P\gamma$ exhibited <5% of the original $P\gamma$ immunoreactivity (25, 26). To remove endogenous cGMP bound to the noncatalytic regulatory sites on $P\alpha\beta$, the $P\alpha\beta$ was incubated at 37°C for 30 min prior to use.

Preparation and Purification of $P\gamma$ and $P\gamma 1-45\text{C}$ —Full-length bovine rod $P\gamma$ or the N-terminal fragment, $P\gamma 1-45\text{C}$, was expressed in *Escherichia coli* using the pET11a expression vector (21) and purified as described previously (4, 25). The total $P\gamma$ concentration was initially determined spectrophotometrically ($\epsilon_{277} = 7550 \text{ cm}^{-1}$) and verified by assaying its inhibitory activity (26); these two estimates varied by <10%. The concentration of $P\gamma 1-45$ was measured with a colorimetric protein assay (27). To fluorescently label $P\gamma 1-45\text{C}$ with Lucifer Yellow ($P\gamma 1-45\text{C-LY}$), the procedure of Artemyev *et al.* (20) was used, followed by purification of $P\gamma 1-45\text{C-LY}$ by reversed-phase high pressure liquid chromatography.

Peptide Purification—Following automated peptide synthesis, peptides were cleaved from the resin with anhydrous hydrofluoric acid and lyophilized. Crude, acidic peptides ($P\gamma 55-75$ and $P\gamma 63-87$) were first purified by anion-exchange chromatography using DEAE Sephadex A-25 and a linear NaCl gradient at pH 7.5. Other peptides were initially purified by cation-exchange chromatography on CM Sephadex C25 using a linear NH_4HCO_3 gradient at pH 8.0. All peptides were further purified by reversed-phase high pressure liquid chromatography on a $22 \times 250\text{-mm}$, 300 angstrom C_{18} column (Vydac), using a linear gradient of 30–70% acetonitrile in 0.1% trifluoroacetic acid. After lyophilization, each peptide was resuspended in 10 mM Tris, pH 7.5, and its concentration was determined with the bicinchoninic acid protein assay (27) using bovine serum albumin as a standard.

Analytical Procedures and Data Analysis—The concentration of PDE and its catalytic activity were determined as described in detail elsewhere (25, 26). Bovine serum albumin (250 $\mu\text{g/ml}$) was added when assaying enzyme concentrations in the subnanomolar range to prevent loss of activity. A membrane filtration assay was used to determine the equilibrium and kinetic properties of cGMP binding to high affinity noncatalytic sites on PDE (25, 26). The PDE inhibitor, zaprinast (0.1–1.0 mM), was included in the assay solution to ensure that <10% hydrolysis of [^3H]cGMP occurred. Nonspecific binding was determined as described previously (28). The fluorescence assay of $P\gamma 1-45\text{C-LY}$ binding to $P\alpha\beta$ was conducted in an Aminco-Bowman Series 2 spectrofluorimeter using an excitation wavelength of 430 nm and an emission wavelength of 520 nm (20).

Except where noted, experiments were performed three times, and the results are presented as the means \pm S.E. Nonlinear regression analysis of the data was performed using Sigmaplot 2000 (SPSS, Inc.).

For the results in Figs. 1 and 2, two different curve-fitting equations were used to fit the $P\gamma$ binding data. The first equation represents the standard equilibrium binding equation for a single class of noninteracting sites.

$$B = \frac{B_{\max} \cdot [P\gamma]}{K_D + [P\gamma]} \quad (\text{Eq. 1})$$

where B is the amount of $P\gamma$ bound, B_{\max} is the maximum extent of binding, K_D is the dissociation constant, and the free $P\gamma$ concentration,

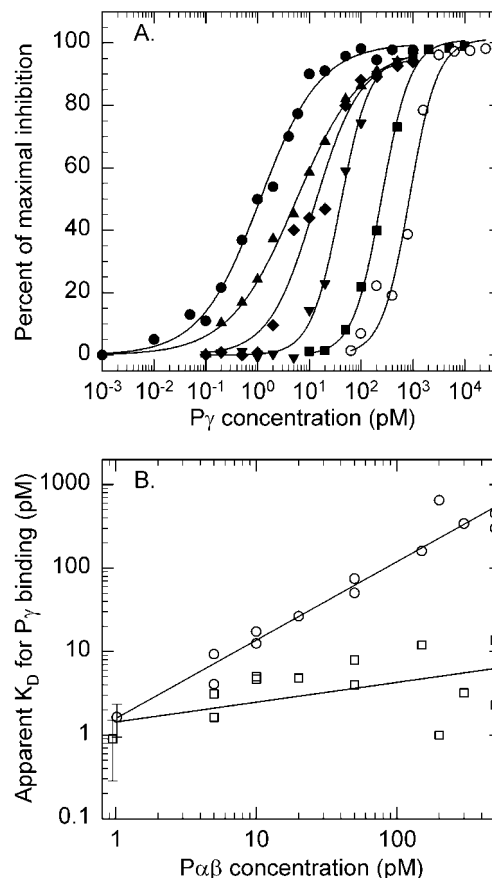


FIG. 1. Inhibition of catalytic activity by $P\gamma$ at various concentrations of $P\alpha\beta$. $P\alpha\beta$ and $P\gamma$ were prepared as described under "Experimental Procedures." A, the ability of increasing amounts of $P\gamma$ to bind to and inhibit hydrolysis of cGMP was determined at the following $P\alpha\beta$ concentrations: 1.0 pM (●), 5.0 pM (▲), 10 pM (◆), 50 pM (▼), 200 pM (■), and 500 pM (○). The substrate concentration was 100 μM cGMP at ≤ 50 pM $P\alpha\beta$ or 2.0 mM at 200 and 500 pM $P\alpha\beta$. The curves represent the fit of the data to Equation 2. B, the affinity of $P\gamma$ binding to $P\alpha\beta$ (apparent K_D) was estimated using either Equation 1 (○) or Equation 2 (□) at each indicated $P\alpha\beta$ concentration. The points represent individual determinations except for 1 pM (mean \pm S.E., $n = 6$).

[$P\gamma$], is assumed to be approximated by the total added $P\gamma$ concentration (*i.e.* [$P\gamma$] \approx [$P\gamma$]_T).

Because the free $P\gamma$ concentration was not experimentally measured, Equation 1 can only be used to estimate the K_D when ligand depletion from solution is not significant. For high affinity binding reactions, this condition is met when the total number of binding sites (P_T) is near the K_D . However, if we substitute the conservation of mass equation ($[P\gamma]_T = B + [P\gamma]$) into Equation 1, we can estimate the K_D for any P_T without having to assume that [$P\gamma$] \approx [$P\gamma$]_T.

$$B = \frac{B_{\max}}{P_T} \left(-x - \frac{\sqrt{x^2 - 4P_T \cdot [P\gamma]_T}}{2} \right) \quad (\text{Eq. 2})$$

where, $x \equiv -K_D - P_T - [P\gamma]_T$. This analytical approach was previously used to study high affinity binding of GTP γ S to transducin (29).

RESULTS

Quantitative Analysis of $P\gamma$ Binding to $P\alpha\beta$ —Given the >100-fold range of reported K_D values for $P\gamma$ binding to PDE6 in the literature (see the Introduction), we suspected that stoichiometric binding of $P\gamma$ to $P\alpha\beta$ was occurring in those instances where the $P\alpha\beta$ concentration exceeded the intrinsic K_D value for the binding reaction. To directly test this, we examined the ability of $P\gamma$ to inhibit catalysis as a function of the $P\alpha\beta$ concentration (Fig. 1A). At $P\alpha\beta$ concentrations ≥ 50 pM, there was a linear increase in the extent of inhibition up to the plateau as the $P\gamma$ concentration was increased; the concentra-

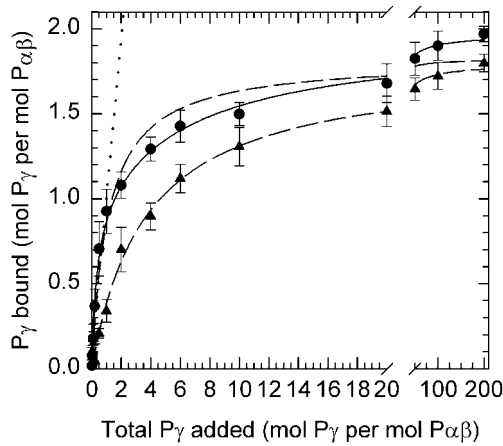


FIG. 2. $P\gamma$ binding affinity at 1 μM $P\alpha\beta$ reveals two classes of binding sites in the presence of cGMP. $P\alpha\beta$ (1.0 μM) was incubated with various concentrations of $P\gamma$ at 4 $^{\circ}\text{C}$ for 10 min, and then the extent of inhibition of cGMP (\bullet , 100 μM concentration; $n = 7$) or cAMP (\blacktriangle , 500 μM concentration; $n = 6$) hydrolysis was determined at 22 $^{\circ}\text{C}$. The cAMP data were well fit as a single class of $P\gamma$ binding sites using either Equation 1 (dashed line, $K_D = 3.7 \pm 0.3$ μM , $B_{\text{max}} = 1.80 \pm 0.03$ mol $P\gamma$ bound per mol $P\alpha\beta$) or Equation 2 ($K_D = 2.6 \pm 0.3$ μM , $B_{\text{max}} = 1.76 \pm 0.04$ $P\gamma/P\alpha\beta$; not shown). The cGMP data did not fit a single site model using either Equation 1 (dashed line) or Equation 2 (not shown), as judged by statistical analysis of the regression. For values of total added $P\gamma$ of ≤ 1.0 , the binding curve fit a linear model (dotted line), consistent with stoichiometric binding ($K_D < 1$ μM) of 1 mol $P\gamma$ /mol $P\alpha\beta$ in the presence of cGMP. A two-site model was also used (by extension of Equation 1) to fit the entire data set (solid line) and resolved the binding curve into two classes of sites with $K_{D1} = 0.3 \pm 0.1$ μM and $K_{D2} = 6.6 \pm 2.3$ μM .

tion of $P\gamma$ needed to attain $>90\%$ inhibition was approximately twice the concentration of $P\alpha\beta$. This behavior represents a titration phenomenon in which added $P\gamma$ stoichiometrically binds to $P\alpha\beta$ with very high affinity until essentially all of the binding sites are occupied (2 mol $P\gamma$ /mol $P\alpha\beta$). At $P\alpha\beta$ concentrations ≤ 10 μM , the inhibition curve departed from stoichiometric behavior, and an excess of $P\gamma$ was needed to fully inhibit the enzyme (Fig. 1A).

The $P\gamma$ binding data in Fig. 1A were analyzed using two equations for equilibrium binding of $P\gamma$ to $P\alpha\beta$. The first approach (Equation 1) assumed that the concentration of free $P\gamma$, $[P\gamma]$, was approximately equal to the total added $P\gamma$ concentration, $[P\gamma]_T$ (i.e. no ligand depletion). When Equation 1 was used to estimate the binding affinity of $P\gamma$ at each concentration of $P\alpha\beta$ tested, we found that the value of the apparent K_D increased in direct proportion to the concentration of $P\alpha\beta$. (Fig. 1B, circles). For example, at 1 μM $P\alpha\beta$, the calculated K_D for $P\gamma$ binding was 1.6 μM , whereas at a concentration of 500 μM $P\alpha\beta$, the curve fitting to Equation 1 gave an apparent K_D of 300 μM .

We re-examined the $P\gamma$ binding data with Equation 2 (which is not constrained by the assumption that $[P\gamma] = [P\gamma]_T$) to estimate the apparent K_D for $P\gamma$ binding. Within the concentration range of 1–500 μM $P\alpha\beta$, the calculated K_D showed little dependence on the $P\alpha\beta$ concentration. The convergence of the two estimates for the apparent K_D as the $P\alpha\beta$ concentration was lowered to 1 μM indicated that both Equation 1 and Equation 2 returned similar estimates when $P_T \leq K_D$ and when the free $P\gamma$ concentration could be approximated as the total $P\gamma$ concentration. We conclude that the most reliable condition for determining the binding affinity of $P\gamma$ is when the $P\alpha\beta$ concentration is in the low μM range.

Heterogeneity in $P\gamma$ Binding to $P\alpha\beta$ —Closer examination of the results at the lowest $P\alpha\beta$ concentration we could easily test (1 μM) indicated that the two $P\gamma$ binding sites on $P\alpha\beta$ were not identical when we assayed $P\gamma$ inhibition of cGMP hydrolysis

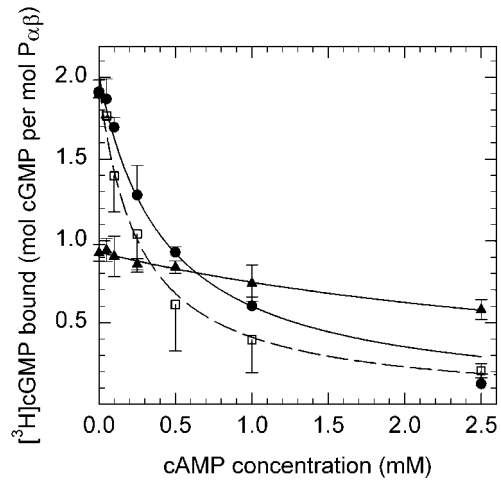


FIG. 3. cAMP binding affinity for the noncatalytic sites of bovine rod $P\alpha\beta$ in the absence of $P\gamma$ or upon addition of $P\gamma$ or $P\gamma 1-45$. 1 μM [^3H]cGMP and the indicated concentrations of cAMP were added to 10 nM $P\alpha\beta$ in the absence of $P\gamma$ (\blacktriangle) or following preincubation with 20 nM $P\gamma$ (\bullet) or 10 μM $P\gamma 1-45$ (\square , mean \pm range for $n = 2$). The ability of cAMP to compete with [^3H]cGMP binding to noncatalytic sites was determined by filter binding, and the data were fit to a single class of noninteracting sites to obtain the following $K_{1/2}$ and B_{max} values, respectively: $P\alpha\beta$, 4.0 mM, 0.9 cGMP/ $P\alpha\beta$; $P\alpha\beta + P\gamma$, 0.4 mM, 2.0 cGMP/ $P\alpha\beta$; $P\alpha\beta + P\gamma 1-45$, 0.3 mM, 2.0 cGMP/ $P\alpha\beta$. The K_D for cAMP binding was calculated from the $K_{1/2}$ value (59) using $K_D = 60$ nM for cGMP binding.

(Fig. 2, circles). When 1 μM $P\alpha\beta$ was incubated with up to 1 mol $P\gamma$ /mol $P\alpha\beta$, stoichiometric binding of $P\gamma$ to $P\alpha\beta$ was observed. This is evident from the fact that the data fit a straight line for the first 50% of the binding curve (Fig. 2, dotted line). After binding 1.0 mol $P\gamma$ /mol $P\alpha\beta$, the remaining $P\gamma$ binding sites required an excess of free $P\gamma$ to fully inhibit $P\alpha\beta$. Attempts to fit the entire binding curve to Equation 1 (Fig. 2, upper dashed line) or Equation 2 failed to generate statistically valid regression coefficients; therefore we fit the data to a modified form of Equation 1 that included two independent classes of binding sites. This approach gave the best fit to the experimental data (Fig. 2, solid line) and resolved two classes of $P\gamma$ binding sites with K_D values of 0.3 and 7 μM . (The 0.3 μM value is the upper limit for the higher affinity K_D . Because this site exhibits titration behavior, the true binding affinity may be greater than the curve-fitting estimate.) Note that the data cannot distinguish between the two independent classes of $P\gamma$ binding sites and a model in which the first $P\gamma$ to bind reduces the binding affinity of $P\alpha\beta$ for the second $P\gamma$ (negative cooperativity).

cGMP Binding to Noncatalytic Sites on $P\alpha\beta$ Is Responsible for $P\gamma$ Binding Heterogeneity—We have previously demonstrated that bovine rod $P\alpha\beta$ (in the absence of $P\gamma$) contains high ($K_D = 60$ nM) and low affinity ($K_D > 1$ μM) cGMP binding sites and that the low affinity site is restored to its high affinity state upon $P\gamma$ addition (25). We hypothesized that the $P\gamma$ binding heterogeneity in Fig. 2 might result from heterogeneity in cGMP binding to the noncatalytic sites. To test this, we needed to measure $P\gamma$ binding when the noncatalytic sites are not occupied with cGMP. cAMP is an alternate substrate for PDE6 catalysis and binds with negligible affinity to amphibian PDE6 ($K_D > 40$ mM) (30). Fig. 3 (triangles) demonstrates that cAMP is able to weakly bind to bovine $P\alpha\beta$, as judged by its ability to compete with cGMP binding to the one high affinity site present on $P\alpha\beta$ (25). Assuming simple competition between cGMP and cAMP binding, cAMP binds to the high affinity noncatalytic site with a K_D of ~ 200 μM .

When we re-examined the binding affinity of $P\gamma$ to $P\alpha\beta$ in the

TABLE I
Kinetic parameters for cyclic nucleotide hydrolysis by bovine rod $P\alpha\beta$

$P\alpha\beta$ was depleted of endogenous, bound cGMP by incubation at 37 °C for 30 min. 5 μM $P\alpha\beta$ (for cGMP as substrate) or 50 μM $P\alpha\beta$ (for cAMP measurements) was added to 0.1–2000 μM cGMP or 15 μM to 60 mM cAMP, and the initial rate of hydrolysis was determined.

Condition	K_m μM	k_{cat} s^{-1}	k_{cat}/K_m $\text{M}^{-1} \text{s}^{-1}$	Hill coefficient
cGMP substrate	14 ± 1.0	5440 ± 80	3.9×10^8	0.9 ± 0.1
cAMP substrate	910 ± 100	3060 ± 100	3.4×10^6	0.9 ± 0.1
cAMP substrate + cGMP occupying noncatalytic sites ^a	830 ± 60	3160 ± 70	3.8×10^6	1.0 ± 0.1

^a To load cGMP on the noncatalytic sites of $P\alpha\beta$, 200 nM $P\alpha\beta$ was first incubated with 5 μM cGMP, 100 μM zaprinast, and 10 μM P γ 1–45. To remove unbound low molecular weight compounds, the $P\alpha\beta$ was concentrated by ultrafiltration. The $P\alpha\beta$ was washed three times by resuspending in buffer (containing P γ 1–45) and reconcentrating. The final $P\alpha\beta$ preparation contained 1.1–1.6 mol cGMP bound per mol $P\alpha\beta$.

presence of 500 μM cAMP, we found that P γ binds to $P\alpha\beta$ with a single K_D value of 3 μM (Fig. 2, triangles). No evidence of binding site heterogeneity or cooperativity was evident when P γ interaction with $P\alpha\beta$ was assayed based on its inhibition of cAMP hydrolysis. This implies that cAMP binding to noncatalytic sites does not affect P γ binding to $P\alpha\beta$. In contrast, binding of cGMP to noncatalytic sites induces an allosteric transition that increases P γ binding affinity ≥ 10 -fold to one site on $P\alpha\beta$. The other P γ binding site maintains an affinity for $P\alpha\beta$ similar to the K_D observed when cAMP is present.

Lack of Direct Allosteric Communication between the Catalytic and Noncatalytic Sites on Bovine $P\alpha\beta$ —Because cGMP binding induces a conformational change in $P\alpha\beta$ that enhances P γ affinity, we hypothesized that the GAF domain might also allosterically regulate hydrolytic activity in the catalytic domain (in analogy to the cGMP-stimulated PDE, PDE2 (31, 32)). To test this, we compared the kinetic parameters of $P\alpha\beta$ using cGMP or cAMP as the substrate. Table I shows that when cGMP is the substrate, $P\alpha\beta$ achieves a catalytic efficiency ($k_{\text{cat}}/K_m = 4 \times 10^8 \text{ M}^{-1} \text{ s}^{-1}$) approaching the diffusion-controlled limit for a bimolecular collision. PDE6 has a 100-fold greater specificity for cGMP compared with cAMP, as judged by the decrease in the k_{cat}/K_m value when cAMP is the substrate. Most of the reduction in substrate specificity for cAMP can be ascribed to the 65-fold increase in its K_m value (Table I). For both cGMP and cAMP, no cooperativity could be detected (Table I), but this is not unexpected because the high affinity noncatalytic site on $P\alpha\beta$ is occupied over most of the concentration range we were able to test.

To directly test whether cGMP occupancy of the noncatalytic sites affected catalysis, we first preincubated $P\alpha\beta$ with cGMP and the N-terminal half of P γ (P γ 1–45) to load cGMP onto both noncatalytic sites. (P γ 1–45 has no effect on catalysis of $P\alpha\beta$ (data not shown) but stabilizes high affinity cGMP binding at both noncatalytic sites on $P\alpha\beta$; see below.) The complex of $P\alpha\beta$ with bound P γ 1–45 and cGMP was then incubated with increasing concentrations of cAMP to determine its kinetic parameters. No significant change in K_m , k_{cat} , or the Hill coefficient could be discerned when compared with $P\alpha\beta$ incubated with cAMP alone (Table I). These results confirm and extend previous observations with amphibian PDE6 (33, 34) that no direct allosteric mechanism regulates catalysis via the state of occupancy of the GAF domains on PDE6, as is the case for PDE2 (31, 32). Thus, the differences in the K_m and k_{cat} values for cAMP and cGMP are due to differences in substrate specificity at the active site not on the state of occupancy of the GAF domain.

The N-terminal Half of P γ Binds to $P\alpha\beta$ with Much Greater Affinity than the C-terminal Region—Previous work has documented that two major domains of interaction with $P\alpha\beta$ exist on P γ : the C-terminal residues and the polycationic central region (see the Introduction). To understand how distinct binding domains on P γ contribute to the very high affinity binding

of P γ to $P\alpha\beta$, we assayed the ability of these individual domains of P γ to bind to $P\alpha\beta$. We first assayed the ability of the C-terminal peptide, P γ 63–87, to bind to and inhibit cyclic nucleotide hydrolysis at the active site. Based on previous work (15), we expected that P γ 63–87 would act as a simple competitive inhibitor with respect to cyclic nucleotides. When cAMP is used as substrate, P γ 63–87 acts as a simple competitive inhibitor of catalysis with an inhibition constant (K_I) equal to 3.5 μM (Fig. 4). The affinity of this inhibitory domain is 6 orders of magnitude weaker than the entire P γ molecule ($K_D = 3 \mu\text{M}$), indicating that the N-terminal 62 amino acids most likely contain the major site(s) of high affinity interaction.

To directly measure the binding affinity of the N-terminal half of P γ to $P\alpha\beta$, we assayed the interaction of P γ 1–45 covalently labeled with Lucifer Yellow (P γ 1–45-LY) with $P\alpha\beta$. Fig. 5A demonstrates that either in the absence of cyclic nucleotides or in the presence of cAMP, $P\alpha\beta$ binds to P γ 1–45-LY as a single class of binding sites with a K_D of 68 ± 15 or 62 ± 14 nM, respectively. In both cases, the maximum extent of binding was the same.

To test how the fluorescent probe altered the binding affinity of P γ 1–45, we also tested the effectiveness of P γ 1–45 in restoring high affinity cGMP binding to the low affinity site on $P\alpha\beta$ (25). In the absence of P γ or P γ 1–45, $P\alpha\beta$ is able to bind 1 mol cGMP/mol $P\alpha\beta$ at micromolar levels of [³H]cGMP (Fig. 3, triangles). The addition of increasing amounts of P γ 1–45 in the presence of 600 nM [³H]cGMP stimulates cGMP binding to a second site on $P\alpha\beta$ (Fig. 5B) with a K_D of 80 nM, a value in good agreement with the K_D for binding of P γ 1–45-LY to $P\alpha\beta$.

We conclude that the N-terminal half of P γ (P γ 1–45) binds to $P\alpha\beta$ about 50-fold more tightly than the C-terminal region (P γ 63–87). Furthermore, if each binding domain were to interact with $P\alpha\beta$ independently, the sum of the interaction energies of P γ 1–45 and P γ 63–87 ($K_D = \sim 10^{-13}$ M) would account reasonably well with the measured K_D for full-length P γ .

Relationship between Occupancy of the GAF Domain and P γ Binding Affinity—In Fig. 2, we showed that heterogeneity in P γ binding to $P\alpha\beta$ (assayed by inhibition of cyclic nucleotide hydrolysis) was dependent on the state of occupancy of the noncatalytic sites. The cGMP-dependent enhancement of full-length P γ binding affinity is also observed with the fluorescently labeled N-terminal half of P γ . Fig. 5A shows that P γ 1–45-LY undergoes a 2.3-fold increase in binding affinity, with no significant change in maximum binding, when the GAF domains are occupied by cGMP compared with empty or cAMP-filled sites. Thus, occupancy of the noncatalytic site by cGMP is required to induce the conformational change in $P\alpha\beta$ that enhances P γ binding affinity.

These results and our previous study with bovine rod $P\alpha\beta$ (25) are in accord with a simple reciprocal relationship: cGMP occupancy of the noncatalytic sites enhances P γ affinity to one of its binding sites and, conversely, P γ binding to $P\alpha\beta$ enhances cGMP binding affinity to its low affinity noncatalytic site. Un-

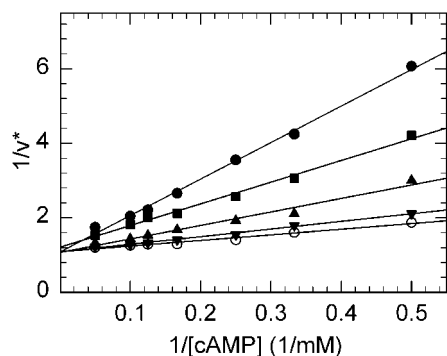


FIG. 4. **Competitive inhibition of P γ 63–87 with cAMP at the active site of P $\alpha\beta$.** P $\alpha\beta$ (2 nM) was incubated with 1.0 (○), 2.0 (▼), 5.0 (▲), 10 (■), or 20 (●) μ M P γ 63–87 for 10 min at room temperature before adding the indicated amounts of cAMP and determining the initial rate. The data were plotted as the reciprocal of the fraction of the maximum rate ($v^* = v/V_{\max}$) versus the reciprocal of the substrate concentration. The inhibition constant (K_i) for P γ 63–87 was calculated to be $2.9 \pm 0.3 \mu$ M from a replot of the slopes versus the corresponding inhibitor concentrations. The data are representative of three experiments with an average K_i of $3.5 \pm 0.5 \mu$ M.

expectedly, this correlation does not apply when cAMP occupies the noncatalytic sites. Fig. 3 shows that the addition of P γ or P γ 1–45 to P $\alpha\beta$ enhances 10-fold the ability of cAMP to compete with cGMP for binding to both noncatalytic sites. This suggests that P γ binding induces a conformational change in P $\alpha\beta$ that enhances the affinity of both cGMP and cAMP for P $\alpha\beta$. However, Fig. 5A reveals that cAMP occupancy of the noncatalytic sites is not sufficient to induce an increase in P γ 1–45-LY binding to P $\alpha\beta$. It appears that cGMP, but not cAMP, is needed to induce a conformational change in P $\alpha\beta$ that enhances P γ binding affinity. This conclusion is supported by experiments with cGMP analogs that show intermediate effects on the relationship between cyclic nucleotide occupancy and enhanced P γ binding affinity.²

Defining the Amino Acid Residues Responsible for High Affinity Interactions of P γ with P $\alpha\beta$ —We prepared a set of synthetic peptides corresponding to various regions of the P γ primary sequence to identify regions of P γ that stabilized high affinity binding of P γ . We first measured the ability of these peptides to compete with full-length, endogenous P γ bound to nonactivated PDE6, as judged by the increase in catalytic activity at the active site. Fig. 6A shows that two peptides, P γ 1–45 and P γ 18–41, were able to compete with full-length P γ to activate PDE6 to 70–80% of its maximal rate and with $K_{1/2}$ values of 1 and 11 μ M, respectively. The P γ 21–46 peptide showed a significant drop in its ability to compete with P γ when compared with P γ 18–41, suggesting that amino acid residues 18–20 may stabilize a peptide conformation of P γ 18–41 that enhances its interaction with P $\alpha\beta$. Several other peptides were able to stimulate cGMP hydrolysis to a limited extent (20–40% activation) and with low affinity ($K_{1/2} = \sim 400$ –500 μ M), including P γ 1–18, P γ 10–30, and P γ 35–56. The peptide P γ 55–75 was completely ineffective in competing with P γ . These results indicate that the interaction of P γ with P $\alpha\beta$ may consist of multiple low affinity sites of interaction along the N-terminal half of the P γ molecule, with high affinity interactions occurring in the region of amino acid residues 18–41.

We showed above that the N-terminal half of P γ , P γ 1–45, could restore high affinity cGMP binding to a low affinity class of noncatalytic sites on P $\alpha\beta$ (Figs. 3 and 5B). To better define this region on P γ , we tested the ability of peptides to bind to P $\alpha\beta$ and restore high affinity cGMP binding to this class of

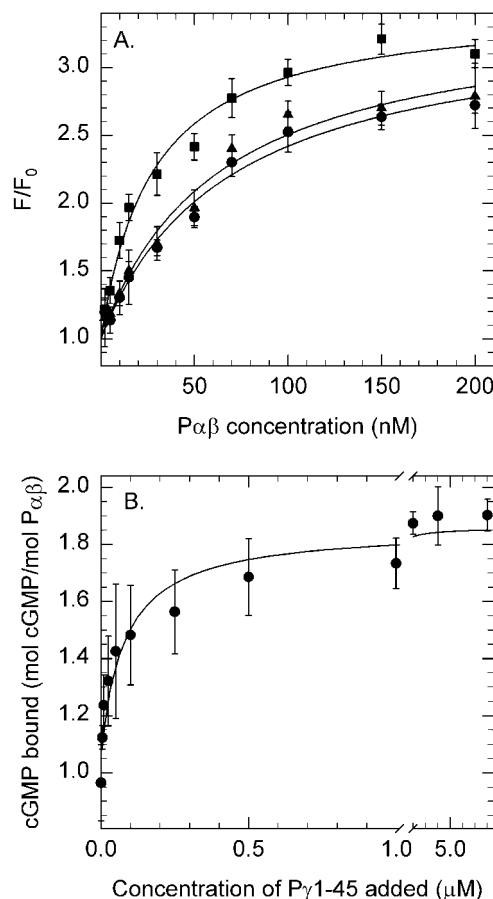


FIG. 5. **High affinity binding of P γ 1–45 to P $\alpha\beta$.** A, the relative increase in fluorescence (F/F_0) of P γ 1–45 labeled with Lucifer Yellow (P γ 1–45-LY) was measured after the addition of the indicated amounts of P $\alpha\beta$. The buffer used for these assays contained 10 mM HEPES, pH 7.8, 100 mM NaCl, 1 mM MgCl₂, 200 μ M zaprinast, and either no nucleotide (●), 10 mM cAMP (▲), or 10 μ M cGMP (■). The curves represent the fit of each data set to a hyperbolic function: no nucleotide, $K_D = 68 \pm 15$ nM, $(F/F_0)_{\max} = 3.3$; cAMP, $K_D = 62 \pm 14$ nM, $(F/F_0)_{\max} = 3.4$; cGMP, $K_D = 28 \pm 5$ nM, $(F/F_0)_{\max} = 3.5$. No evidence for cooperativity was detected using the Hill equation to fit the data. B, the ability of P γ 1–45 to restore high affinity cGMP binding to a low affinity class of noncatalytic sites on P $\alpha\beta$ (10 nM) was measured following incubation of P $\alpha\beta$ with the indicated concentration of P γ 1–45 and 600 nM [³H]cGMP. The data represent the averages of four different experiments, and the curve is the fit of the data to a hyperbolic function ($K_D = 83$ nM; $B_{\max} = 1.9$ mol cGMP bound per mol P $\alpha\beta$).

sites. Fig. 6B shows that P γ 18–41 and P γ 21–46 both fully restored cGMP binding to P $\alpha\beta$ with a binding affinity reduced ~ 10 -fold compared with P γ 1–45. P γ 10–30 was also able to fully restore cGMP binding, but its interaction with P $\alpha\beta$ was 10-fold further reduced. Even though P γ 15–26 failed to interact with P $\alpha\beta$ to restore cGMP binding, the overall results with several other peptides suggest that residues 18–30 of P γ are important in stabilizing P γ binding to P $\alpha\beta$.

We also tested peptides covering amino acids 35–56 of the P γ sequence (Fig. 6B). Although full restoration of cGMP binding could not be observed with P γ 35–56 or smaller peptides, all three peptides showed K_D values in the 20–30 μ M range. The effectiveness of the shortest peptide, P γ 35–41, to stimulate cGMP binding to P $\alpha\beta$ indicates that these residues are important in direct binding to P $\alpha\beta$ and in stabilizing a high affinity conformation of the second noncatalytic site on PDE6.

Although P γ 1–45 has 10-fold higher affinity for P $\alpha\beta$ than P γ 18–41, we could not detect any interaction of the peptide P γ 1–18 with P $\alpha\beta$ in terms of restoring high affinity cGMP binding (Fig. 6B). It is possible that some of the N-terminal

² H. Mou and R. H. Cote, unpublished observations.

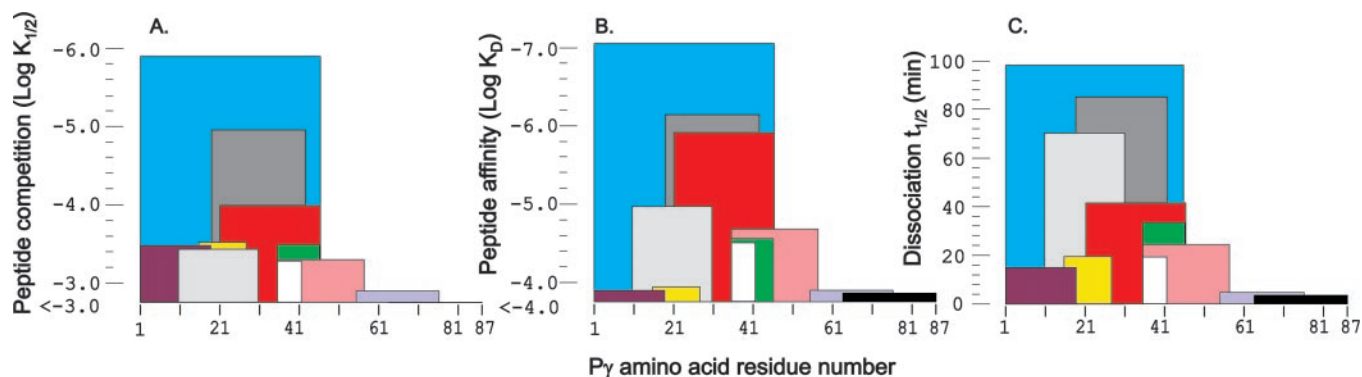


FIG. 6. Ability of P γ peptides to interact with P $\alpha\beta$. A, the catalytic activity of nonactivated PDE6 holoenzyme (5 nM) was tested following incubation of PDE6 with increasing concentrations of P γ peptides. The maximum extent of activation and the $K_{1/2}$ for the P γ peptides were determined by fitting the concentration dependence to a hyperbolic function. The *ordinate* represents the $\log(K_{1/2})$ for each peptide, and the *abscissa* visually depicts each P γ peptide tested. The maximum percentage of activation of cGMP hydrolysis induced by each peptide was: P γ 1–45, 81%; P γ 18–41, 69%; P γ 10–30, 42%; P γ 35–56, 32%; P γ 21–46, 25%; P γ 1–18, 18%; P γ 15–26, 14%; P γ 35–46, 11%; P γ 35–41, 9%; P γ 55–75, <5%. B, the ability of P γ peptides to restore high affinity cGMP binding to low affinity sites on P $\alpha\beta$ was determined as described in the legend to Fig. 5B, and the K_D values are plotted on the *ordinate* on a log scale. The B_{\max} for restoring high affinity binding (percentage of restoration observed with P γ = 100%) was: 100% (P γ , P γ 1–45, P γ 10–30, P γ 18–41), 90% (P γ 21–46), 70% (P γ 35–56, P γ 35–46), 40% (P γ 35–41), and 0% (P γ 1–18, P γ 15–26, P γ 55–75, P γ 63–87). C, the [3 H]cGMP dissociation kinetics were determined at 22 °C by preincubating 5 nM P $\alpha\beta$ with 0.6 μ M [3 H]cGMP and 200 μ M of the indicated P γ peptide until binding equilibrium was attained. Dissociation of bound [3 H]cGMP was initiated by the addition of 2 mM unlabeled cGMP, and the data were fit to a single exponential decay function to determine the $t_{1/2}$ from the equation: $t_{1/2} = 0.693/k_{-1}$, where k_{-1} is the dissociation rate constant.

residues may stabilize a conformation of P γ 1–45 that favors its binding to P $\alpha\beta$ compared with P γ 18–41. Two other peptides, P γ 55–75 and P γ 63–87, completely lacked the ability to restore cGMP binding even at 300 μ M peptide concentrations.

The binding affinity of cGMP for the noncatalytic sites was determined in the presence of 200 μ M of each peptide to examine whether the low and high affinity noncatalytic sites could be distinguished (data not shown). All P γ peptides that were competent to restore cGMP binding to the low affinity sites failed to alter the K_D for cGMP binding (K_D range: 51–63 nM). No evidence for binding site heterogeneity could be detected. We conclude that binding of P γ or central region P γ peptides induces a conformational change in the low affinity noncatalytic site that enhances its affinity for cGMP to a value indistinguishable from the high affinity noncatalytic site.

The restoration of cGMP binding shown in Fig. 6B describes the ability of P γ peptides to act on the low affinity noncatalytic sites on P $\alpha\beta$. To examine both high and low affinity noncatalytic sites, we examined whether P γ peptides could alter the rate of [3 H]cGMP dissociation from the noncatalytic sites of P $\alpha\beta$. Fig. 6C shows that most of the peptides were able to retard the rate of [3 H]cGMP dissociation from the noncatalytic sites. In all instances, the dissociation kinetics were fit to a single exponential loss of [3 H]cGMP binding; no evidence for two distinct classes of sites was evident (*not shown*). As expected, P γ 1–45 most effectively retarded cGMP exchange at both noncatalytic sites on P $\alpha\beta$, causing a 16-fold increase in the half-time for [3 H]cGMP release from noncatalytic sites. The P γ peptides P γ 18–41 and P γ 10–30 also retarded cGMP exchange by greater than 10-fold. Comparison of P γ 18–41 ($t_{1/2} = 84$ min) with P γ 21–46 ($t_{1/2} = 41$ min) supports the importance of amino acid residues 18–20 in stabilizing binding of P γ peptides to P $\alpha\beta$. The P γ peptide, P γ 35–46, is nearly as effective as the larger P γ 21–46 in slowing the rate of cGMP dissociation from P $\alpha\beta$, whereas the 7-amino acid P γ 35–41 also acted to increase the half-time for cGMP dissociation 3-fold.

Two peptides, P γ 55–75 and P γ 63–83, were unable to affect cGMP dissociation compared with P $\alpha\beta$ lacking P γ peptides ($t_{1/2} = 6$ min), in agreement with their inability to restore cGMP binding to low affinity sites (Fig. 6B). The fact that the P γ 1–18 and P γ 15–26 peptides slowed cGMP dissociation \sim 3-fold from the high affinity noncatalytic sites of P $\alpha\beta$ (Fig. 6C) without

being able to restore cGMP binding to the low affinity site (Fig. 6B) suggests that this region of P γ may affect only the high affinity GAF domain of PDE6.

DISCUSSION

This paper shows that P γ binds to two distinct high affinity binding sites on P $\alpha\beta$ when cGMP occupies the noncatalytic sites. Our work also describes the reciprocal allosteric regulation of PDE6 resulting from P γ binding to P $\alpha\beta$ and cGMP binding to high affinity sites in the GAF domains of P $\alpha\beta$. Because no direct allosteric communication between the GAF domains and the active sites is detected, we conclude that the P γ subunit is required to facilitate allosteric communication between the regulatory and catalytic domains of PDE6. Finally, we have mapped regions within the N-terminal half of the molecule that interact with P $\alpha\beta$, some of which induce conformational changes at the GAF domain.

Implications of High Affinity, Two-site P γ Binding to P $\alpha\beta$ for PDE Function—Our quantitative analysis of P γ binding to P $\alpha\beta$ helps to make sense of the wide range of apparent binding affinities reported in the literature. The majority of studies of the P γ affinity for P $\alpha\beta$ have been carried out with concentrations of enzyme much greater than the K_D value for P γ binding. Under these conditions, P γ will bind in a stoichiometric manner (Fig. 1). Even when the appropriate model is applied to the binding data (*i.e.* Equation 2), it is difficult to extract meaningful values for the K_D values. For example, we were unable to satisfactorily fit data obtained at >800 pM P $\alpha\beta$ concentrations to Equation 2, primarily because the estimate of the free P γ concentration is very uncertain.² In previous reports where the PDE concentration was lowered into the picomolar range (5, 6, 34), the binding affinities of P γ for P $\alpha\beta$ were much closer to the values we report. Previous evidence supporting two distinct P γ binding sites on P $\alpha\beta$ has mostly been obtained indirectly, based on heterogeneity in transducin activation of PDE6 (11, 12, 35, 36). However, Berger *et al.* (10) have reported two classes of P γ binding sites on P $\alpha\beta$ when probed with a fluorescently labeled mutant of P γ .

The functional heterogeneity in P γ binding to P $\alpha\beta$ is a consequence of the state of occupancy of the noncatalytic sites with cGMP (Fig. 2)—but not cAMP. Because the membrane-associated bovine rod PDE6 holoenzyme has one exchangeable and

one nonexchangeable cGMP binding site (25), we hypothesize that the very high affinity ($K_D < 1$ pM) $P\gamma$ binding site may correlate with this nonexchangeable cGMP site. This $P\gamma$ binding site associated with the nonexchangeable cGMP site is unlikely to function during visual transduction. Instead, it may serve a structural role in stabilizing the native conformation of the PDE6 holoenzyme. This idea is supported by studies showing that mutations in the GAF domains of PDE6 (Ref. 37; reviewed in Ref. 38) or a disrupted or mutated $P\gamma$ gene (39) can affect the levels of expression and/or activation of PDE6. It might also explain the difficulty in expressing functional PDE6 in various expression systems (40–42) if co-expression of catalytic and $P\gamma$ subunits must occur to properly fold the nascent polypeptide chains of PDE6.

Allosteric Regulation of PDE6 Requires $P\gamma$ to Communicate between the GAF Domain and the Catalytic Domain—In addition to a catalytic domain near the C terminus that is conserved in all members of the vertebrate PDE superfamily, most PDE families contain N-terminal domains that serve regulatory functions. It has been proposed (43) that a common regulatory feature of the N-terminal domain is to alter the inhibitory constraint on catalysis via conformational changes in the catalytic dimer. Almost half of the known PDE families (PDE2, PDE5, PDE6, PDE10, and PDE11) contain two tandem GAF domains (44) that in most cases code for functional, noncatalytic cGMP binding sites. For PDE2 and PDE5, binding of cGMP to the GAF domain induces a conformational change in the catalytic dimer that either directly or indirectly stimulates catalysis (31, 32, 45, 46). For PDE6, we show that loading the GAF domain with cGMP has no direct influence on PDE6 kinetic parameters (Table I).

Nonetheless, cGMP binding to the GAF domain of PDE6 does induce a conformational change in the catalytic dimer. Occupancy of the noncatalytic sites enhances the interaction of $P\gamma$ (Fig. 2) or $P\gamma$ 1–45 (Fig. 5A) to the catalytic dimer. This effect is specific for cGMP (Fig. 5A). Conversely, the addition of $P\gamma$ to bovine rod $P\alpha\beta$ enhances cyclic nucleotide binding affinity to the noncatalytic sites (Fig. 3) in a reciprocal manner. For cGMP, $P\gamma$ acts to restore high affinity binding to a low affinity class of sites on bovine $P\alpha\beta$; the other, high affinity class of cGMP sites undergoes no change in affinity (25). For cAMP, addition of $P\gamma$ or $P\gamma$ 1–45 to $P\alpha\beta$ increases the binding affinity 10-fold to both noncatalytic sites on $P\alpha\beta$ (Fig. 3).

We conclude that unlike PDE2 or PDE5, the GAF domain in the PDE6 catalytic subunit is allosterically uncoupled from its catalytic domain unless $P\gamma$ is bound to bridge the two domains. Furthermore, the heterogeneity in $P\gamma$ binding to $P\alpha\beta$ suggests that only one $P\gamma$ binding site on $P\alpha\beta$ is sensitive to cGMP occupancy of the noncatalytic sites. Future efforts will identify which catalytic subunit contains the cGMP-sensitive $P\gamma$ binding site and the high affinity noncatalytic site on $P\alpha\beta$.

$P\gamma$ Is a Multi-functional Subunit with Several Sites of Interaction with the PDE6 Transduction Complex—The $P\gamma$ subunit of PDE6 contains within its 87-amino acid sequence numerous sites of interactions with $P\alpha\beta$, transducin, RGS-9, and perhaps other proteins (see the Introduction). In this study, we have focused on $P\gamma$ - $P\alpha\beta$ interactions and find that the N-terminal half of $P\gamma$ binds 50-fold more tightly to the catalytic dimer than the C-terminal region ($P\gamma$ 63–87). This high affinity binding domain in the region of residues 18–41 of $P\gamma$ explains why α_t^* activation of the PDE6 holoenzyme sometimes displaces the inhibitory constraint of $P\gamma$ without causing complete dissociation of $P\gamma$ from $P\alpha\beta$ (5, 47). The correlation of $P\gamma$ dissociation from transducin-activated PDE with loss of cGMP from the GAF domain (12) also makes sense based on the reduced binding affinity of $P\gamma$ or $P\gamma$ 1–45 in the absence of cGMP (Figs. 2 and 5).

Within the central region of the $P\gamma$ subunit, amino acids 18–20 and 35–41 contribute to stabilizing $P\gamma$ binding to $P\alpha\beta$ (Fig. 6). Other $P\gamma$ interaction sites probably exist within this polycationic region that went undetected with our selected peptides, including potential sites of regulation via phosphorylation at Thr²² and/or Thr³⁵ (48–50) or via ADP-ribosylation at Arg³³ or Arg³⁶ (51).

Our results demonstrate that the N-terminal 18 amino acids of $P\gamma$ play no direct role in inhibiting catalysis or stimulating high affinity cGMP binding to $P\alpha\beta$ (Fig. 6), contrary to a previous study (52). However, the N terminus of $P\gamma$ probably contains weak sites of interaction with $P\alpha\beta$ and may help stabilize a high affinity conformation of the 18–41 region of $P\gamma$.

Significantly, the one peptide that shows no detectable interaction with $P\alpha\beta$, namely $P\gamma$ 55–75, contains a major site of interaction with activated transducin, α_t^* (see the Introduction). A recent structural determination of the interaction of the C-terminal half of $P\gamma$ with α_t^* has shown that α_t^* binds to several residues in the vicinity of Trp⁷⁰ of $P\gamma$ to cause the displacement of the C-terminal residues of $P\gamma$ known to block the active site (22).

Summary—Our results extend previous models postulating two major sites of interaction between PDE6 and activated transducin, both of which are mediated through the inhibitory $P\gamma$ subunit. The extreme C terminus of $P\gamma$ functions to block catalysis at the active site but has relatively low affinity for $P\alpha\beta$. It is the high affinity interactions of the central, polycationic region of $P\gamma$ (particularly residues 18–41) that stabilize binding to $P\alpha\beta$, thereby insuring that a very small fraction of PDE6 holoenzyme is catalytically active prior to light activation. High levels of cGMP in dark-adapted photoreceptor cells result in saturation of the noncatalytic sites on PDE6, further enhancing $P\gamma$ affinity to one binding site on the PDE6 holoenzyme. Upon activation of the phototransduction cascade, binding of activated transducin to the PDE6 holoenzyme, specifically in the vicinity of Trp⁷⁰ of $P\gamma$, is sufficient to displace the $P\gamma$ C terminus and cause activation at one active site on $P\alpha\beta$. (The very high affinity $P\gamma$ binding site ($K_D < \text{pM}$) when cGMP is present likely prevents α_t^* displacement of $P\gamma$ at the second active site (11, 12).) At early times following light stimulation, α_t^* remains associated with the PDE6 holoenzyme and does not physically dissociate as a α_t^* - $P\gamma$ complex. Following PDE6 activation, cGMP levels in the outer segment drop and remain low until the inactivation process reinhibits PDE6. The positive cooperativity between the GAF domains and the central region of $P\gamma$ suggests that a sustained lowering of cGMP levels (e.g. during light adaptation) will lead to cGMP dissociation and a lowered $P\gamma$ affinity for $P\alpha\beta$. This cGMP-dependent allosteric transition could cause the multi-functional $P\gamma$ subunit to become available to interact with RGS-9 to facilitate an enhanced GTPase rate on α_t^* , consistent with biochemical and structural studies (22, 53–55).

Although homology modeling of the GAF domain (56) and the catalytic domain (57, 58) of PDE complement recent structural information on $P\gamma$ binding to α_t^* (22), we still lack crystal structures revealing the interactions of each $P\gamma$ molecule with the α and β subunits of the rod PDE6 heterodimer. The present study provides the biochemical basis for understanding how the central and C-terminal domains of $P\gamma$ bridge the regulatory and catalytic domains of the rod PDE6 heterodimer to control the magnitude and duration of PDE activation during visual excitation, recovery, and light adaptation.

REFERENCES

1. Pfister, C., Bennett, N., Bruckert, F., Catty, P., Clerc, A., Pagès, F., and Deterre, P. (1993) *Cell. Signal.* **5**, 235–251
2. Pugh, E. N., Jr., and Lamb, T. D. (1993) *Biochim. Biophys. Acta* **1141**, 111–149
3. Bownds, M. D., and Arshavsky, V. Y. (1995) *Behav. Brain Sci.* **18**, 415–424

4. Artemyev, N. O., Arshavsky, V. Y., and Cote, R. H. (1998) *Methods* **14**, 93–104
5. Wensel, T. G., and Stryer, L. (1986) *Prot. Struct. Funct. Genet.* **1**, 90–99
6. Hamilton, S. E., Prusti, R. K., Bentley, J. K., Beavo, J. A., and Hurley, J. B. (1993) *FEBS Lett.* **318**, 157–161
7. Skiba, N. P., Artemyev, N. O., and Hamm, H. E. (1995) *J. Biol. Chem.* **270**, 13210–13215
8. Otto-Bruc, A., Antonny, B., Vuong, T. M., Chardin, P., and Chabre, M. (1993) *Biochemistry* **32**, 8636–8645
9. Yamazaki, A., Yamazaki, M., Bondarenko, V. A., and Matsumoto, H. (1996) *Biochem. Biophys. Res. Commun.* **222**, 488–493
10. Berger, A. L., Cerione, R. A., and Erickson, J. W. (1999) *Biochemistry* **38**, 1293–1299
11. Melia, T. J., Malinski, J. A., He, F., and Wensel, T. G. (2000) *J. Biol. Chem.* **275**, 3535–3542
12. Norton, A. W., D'Amours, M. R., Grazio, H. J., Hebert, T. L., and Cote, R. H. (2000) *J. Biol. Chem.* **275**, 38611–38619
13. Lipkin, V. M., Dumler, I. L., Muradov, K. G., Artemyev, N. O., and Etingof, R. N. (1988) *FEBS Lett.* **234**, 287–290
14. Brown, R. L. (1992) *Biochemistry* **31**, 5918–5925
15. Granovsky, A. E., Natochin, M., and Artemyev, N. O. (1997) *J. Biol. Chem.* **272**, 11686–11689
16. Artemyev, N. O., and Hamm, H. E. (1992) *Biochem. J.* **283**, 273–279
17. Takemoto, D. J., Hurt, D., Oppert, B., and Cunnick, J. (1992) *Biochem. J.* **281**, 637–643
18. Lipkin, V. M., Bondarenko, V. A., Zagranichny, V. E., Dobrynina, L. N., Muradov, K. G., and Natochin, M. Y. (1993) *Biochim. Biophys. Acta* **1176**, 250–256
19. Natochin, M., and Artemyev, N. O. (1996) *J. Biol. Chem.* **271**, 19964–19969
20. Artemyev, N. O., Rarick, H. M., Mills, J. S., Skiba, N. P., and Hamm, H. E. (1992) *J. Biol. Chem.* **267**, 25067–25072
21. Slepak, V. Z., Artemyev, N. O., Zhu, Y., Dumke, C. L., Sabacan, L., Sondek, J., Hamm, H. E., Bownds, M. D., and Arshavsky, V. Y. (1995) *J. Biol. Chem.* **270**, 14319–14324
22. Slep, K. C., Kercher, M. A., He, W., Cowan, C. W., Wensel, T. G., and Sigler, P. B. (2001) *Nature* **409**, 1071–1077
23. Tsang, S. H., Burns, M. E., Calvert, P. D., Gouras, P., Baylor, D. A., Goff, S. P., and Arshavsky, V. Y. (1998) *Science* **282**, 117–121
24. Skiba, N. P., Bae, H., and Hamm, H. E. (1996) *J. Biol. Chem.* **271**, 413–424
25. Mou, H., Grazio, H. J., Cook, T. A., Beavo, J. A., and Cote, R. H. (1999) *J. Biol. Chem.* **274**, 18813–18820
26. Cote, R. H. (2000) *Methods Enzymol.* **315**, 646–672
27. Smith, P. K., Krohn, R. I., Hermanson, G. T., Mallia, A. K., Gartner, F. H., Provenzano, M. D., Fujimoto, E. K., Goeke, N. M., Olson, B. J., and Klenk, D. C. (1985) *Anal. Biochem.* **150**, 76–85
28. Cote, R. H., and Brunnock, M. A. (1993) *J. Biol. Chem.* **268**, 17190–17198
29. Malinski, J. A., Zera, E. M., Angleson, J. K., and Wensel, T. G. (1996) *J. Biol. Chem.* **271**, 12919–12924
30. Hebert, M. C., Schwede, F., Jastorff, B., and Cote, R. H. (1998) *J. Biol. Chem.* **273**, 5557–5565
31. Martins, T. J., Mumby, M. C., and Beavo, J. A. (1982) *J. Biol. Chem.* **257**, 1973–1979
32. Yamamoto, T., Manganiello, V. C., and Vaughan, M. (1983) *J. Biol. Chem.* **258**, 12526–12533
33. Arshavsky, V. Y., Dumke, C. L., and Bownds, M. D. (1992) *J. Biol. Chem.* **267**, 24501–24507
34. D'Amours, M. R., and Cote, R. H. (1999) *Biochem. J.* **340**, 863–869
35. Bennett, N., and Clerc, A. (1989) *Biochem. J.* **28**, 7418–7424
36. Bruckert, F., Catty, P., Deterre, P., and Pfister, C. (1994) *Biochemistry* **33**, 12625–12634
37. Gal, A., Orth, U., Baehr, W., Schwinger, E., and Rosenberg, T. (1994) *Nat. Genet.* **7**, 64–68
38. Dryja, T. P., Rucinski, D. E., Chen, S. H., and Berson, E. L. (1999) *Invest. Ophthalmol. Vis. Sci.* **40**, 1859–1865
39. Tsang, S. H., Gouras, P., Yamashita, C. K., Kjeldbye, H., Fisher, J., Farber, D. B., and Goff, S. P. (1996) *Science* **272**, 1026–1029
40. Piriev, N. I., Yamashita, C., Samual, G., and Farber, D. B. (1993) *Proc. Natl. Acad. Sci. U. S. A.* **90**, 9340–9344
41. Qin, N., and Baehr, W. (1994) *J. Biol. Chem.* **269**, 3265–3271
42. Granovsky, A. E., Natochin, M., McEntaffer, R. L., Haik, T. L., Francis, S. H., Corbin, J. D., and Artemyev, N. O. (1998) *J. Biol. Chem.* **273**, 24485–24490
43. Conti, M. (2000) *Mol. Endocrinol.* **14**, 1317–1327
44. Aravind, L., and Ponting, C. P. (1997) *Trends Biochem. Sci.* **22**, 458–459
45. Burns, F., Rodger, I. W., and Pyne, N. J. (1992) *Biochem. J.* **283**, 487–491
46. Corbin, J. D., Turko, I. V., Beasley, A., and Francis, S. H. (2000) *Eur. J. Biochem.* **267**, 2760–2767
47. Clerc, A., and Bennett, N. (1992) *J. Biol. Chem.* **267**, 6620–6627
48. Tsuboi, S., Matsumoto, H., Jackson, K. W., Tsujimoto, K., Williams, T., and Yamazaki, A. (1994) *J. Biol. Chem.* **269**, 15016–15023
49. Xu, L. X., Tanaka, Y., Bondarenko, V. A., Matsuura, I., Matsumoto, H., Yamazaki, A., and Hayashi, F. (1998) *Biochemistry* **37**, 6205–6213
50. Matsuura, I., Bondarenko, V. A., Maeda, T., Kachi, S., Yamazaki, M., Usukura, J., Hayashi, F., and Yamazaki, A. (2000) *J. Biol. Chem.* **275**, 32950–32957
51. Bondarenko, V. A., Desai, M., Dua, S., Yamazaki, M., Amin, R. H., Yousif, K. K., Kinumi, T., Ohashi, M., Komori, N., Matsumoto, H., Jackson, K. W., Hayashi, F., Usukura, J., Lipkin, V. M., and Yamazaki, A. (1997) *J. Biol. Chem.* **272**, 15856–15864
52. Yamazaki, A., Bondarenko, V. A., Dua, S., Yamazaki, M., Usukura, J., and Hayashi, F. (1996) *J. Biol. Chem.* **271**, 32495–32498
53. Arshavsky, V. Y., and Bownds, M. D. (1992) *Nature* **357**, 416–417
54. Calvert, P. D., Ho, T. W., LeFebvre, Y. M., and Arshavsky, V. Y. (1998) *J. Gen. Physiol.* **111**, 39–51
55. He, W., Cowan, C. W., and Wensel, T. G. (1998) *Neuron* **20**, 95–102
56. Ho, Y.-S. J., Burden, L. M., and Hurley, J. H. (2000) *EMBO J.* **19**, 5288–5299
57. Xu, R. X., Hassell, A. M., Vanderwall, D., Lambert, M. H., Holmes, W. D., Luther, M. A., Rocque, W. J., Milburn, M. V., Zhao, Y., Ke, H., and Nolte, R. T. (2000) *Science* **288**, 1822–1825
58. Granovsky, A. E., and Artemyev, N. O. (2000) *J. Biol. Chem.* **275**, 41258–41262
59. Cheng, Y.-C., and Prusoff, W. H. (1973) *Biochem. Pharmacol.* **22**, 3099–3108